AGU PUBLICATIONS

Global Biogeochemical Cycles

RESEARCH ARTICLE

10.1002/2014GB004826

Key Points:
- Models largely agree on the sign of the carbon flux response to climate extremes
- Models are uncertain in the carbon flux response to heat waves in boreal forests
- Droughts and heat waves strongly compound each other in their impact on C fluxes

Correspondence to:
J. Zscheischler,
jzsch@bgc-jena.mpg.de

Citation:
Zscheischler, J., et al. (2014), Impact of large-scale climate extremes on biospheric carbon fluxes: An intercomparison based on MsTMIP data, *Global Biogeochem. Cycles*, *28*, doi:10.1002/2014GB004826.

Received 7 FEB 2014
Accepted 9 MAY 2014
Accepted article online 13 MAY 2014

Impact of large-scale climate extremes on biospheric carbon fluxes: An intercomparison based on MsTMIP data

Jakob Zscheischler[1,2,3], Anna M. Michalak[2], Christopher Schwalm[4], Miguel D. Mahecha[1], Deborah N. Huntzinger[4], Markus Reichstein[1], Gwenaëlle Berthier[5], Philippe Ciais[5], Robert B. Cook[6], Bassil El-Masri[7], Maoyi Huang[8], Akihiko Ito[9], Atul Jain[7], Anthony King[6], Huimin Lei[10], Chaoqun Lu[11], Jiafu Mao[7], Shushi Peng[5,12], Benjamin Poulter[13], Daniel Ricciuto[6], Xiaoying Shi[7], Bo Tao[11], Hanqin Tian[11], Nicolas Viovy[5], Weile Wang[14], Yaxing Wei[7], Jia Yang[11], and Ning Zeng[15]

[1]Max Planck Institute for Biogeochemistry, Jena, Germany, [2]Department of Global Ecology, Carnegie Institution for Science, Stanford, California, USA, [3]Max Planck Institute for Intelligent Systems, Tübingen, Germany, [4]School of Earth Sciences and Environmental Sustainability, Northern Arizona University, Flagstaff, Arizona, USA, [5]Laboratoire des Sciences du Climat et de l'Environnement, Gif-sur-Yvette, France, [6]Environmental Sciences Division, Oak Ridge National Laboratory, Oak Ridge, Tennessee, USA [7]Department for Atmospheric Sciences, University of Illinois at Urbana-Champaign, Urbana, Illinois, USA, [8]Atmospheric and Global Change Division, Pacific Northwest National Laboratory, Richland, Washington, USA, [9]National Institute for Environmental Studies, Tsukuba, Japan [10]Department of Hydraulic Engineering, Tsinghua University, Beijing, China [11]International Center for Climate and Global Change Research and School of Forestry and Wildlife Sciences, Auburn University, Auburn, Alabama, USA [12]Laboratoire de Glaciologie et Géophysique de l'Environnement, CNRS and Université Grenoble Alpes, Grenoble, France, [13]Department of Ecology, Montana State University, Bozeman, Montana, USA, [14]Ames Research Center, National Aeronautics and Space Administration, Moffett Field, California, USA, [15]Department of Atmospheric and Oceanic Science, University of Maryland, College Park, Maryland, USA

Abstract Understanding the role of climate extremes and their impact on the carbon (C) cycle is increasingly a focus of Earth system science. Climate extremes such as droughts, heat waves, or heavy precipitation events can cause substantial changes in terrestrial C fluxes. On the other hand, extreme changes in C fluxes are often, but not always, driven by extreme climate conditions. Here we present an analysis of how extremes in temperature and precipitation, and extreme changes in terrestrial C fluxes are related to each other in 10 state-of-the-art terrestrial carbon models, all driven by the same climate forcing. We use model outputs from the North American Carbon Program Multi-scale Synthesis and Terrestrial Model Intercomparison Project (MsTMIP). A global-scale analysis shows that both droughts and heat waves translate into anomalous net releases of CO_2 from the land surface via different mechanisms: Droughts largely decrease gross primary production (GPP) and to a lower extent total respiration (TR), while heat waves slightly decrease GPP but increase TR. Cold and wet periods have a smaller opposite effect. Analyzing extremes in C fluxes reveals that extreme changes in GPP and TR are often caused by strong shifts in water availability, but for extremes in TR shifts in temperature are also important. Extremes in net CO_2 exchange are equally strongly driven by deviations in temperature and precipitation. Models mostly agree on the sign of the C flux response to climate extremes, but model spread is large. In tropical forests, C cycle extremes are driven by water availability, whereas in boreal forests temperature plays a more important role. Models are particularly uncertain about the C flux response to extreme heat in boreal forests.

1. Introduction

Environmental conditions such as temperature and water availability are strongly interlinked with terrestrial carbon fluxes. Overall, the terrestrial biosphere is currently providing a negative feedback to a warming world [*Friedlingstein et al.*, 2006]. However, the nature and magnitude of most feedback mechanisms between the atmosphere and biosphere are still uncertain. Warmer temperatures, for instance, often increase terrestrial gross carbon uptake [*Beer et al.*, 2010] but also soil respiration [*Mahecha et al.*, 2010], resulting in a largely uncertain net carbon-cycle response to climate change. The last generation of coupled climate-carbon models largely disagreed as to whether the terrestrial biosphere will act as a sink or a source of carbon to the atmosphere in future [*Friedlingstein et al.*, 2006]. This uncertainty still holds for the more recent model runs collected in the Coupled Model Intercomparison Project Phase 5 (CMIP5) [*Ahlström et al.*, 2012; *Jones et al.*, 2013].

Climate extremes such as droughts, heat waves, or intense precipitation events can significantly affect carbon fluxes [*Reichstein et al.*, 2013]. Their impacts might, in some cases, temporarily reverse the effect of years of carbon sequestration [*Ciais et al.*, 2005]. However, fast recovery can partly offset instantaneous impacts of climate extremes and disturbance events [*Amiro et al.*, 2010]. Identifying extremes directly in variables describing the state of the biosphere such as fraction of absorbed photosynthetically active radiation or enhanced vegetation index can lead to new insights about the relationship between extreme climate drivers on the one hand and extreme responses on the other [*Zscheischler et al.*, 2013; *Reichstein et al.*, 2013]. It has recently been shown that extremes in gross primary production (GPP) are the main driver of GPP's interannual variability at the global [*Zscheischler et al.*, 2014a] and the continental scale [*Zscheischler et al.*, 2014b], with water scarcity driving most of the negative extreme events. While droughts often significantly influence carbon uptake, higher water availability can also mitigate the impacts of heat waves [*Bauweraerts et al.*, 2014]. In a warming climate, the intensity and frequency of climate extremes and their geographical distribution will change substantially [*Seneviratne et al.*, 2012; *Sillmann et al.*, 2013; *Fischer et al.*, 2013], suggesting concurrent changes in carbon cycle variability.

So far little attention has been given to model performance during extreme events. *Keenan et al.* [2012] discuss model performance and lagged impacts in response to one extreme event within a model-data intercomparison study. *Zscheischler et al.* [2014a, 2014b] analyze GPP extreme events on four different GPP data sets and find that droughts are the main driver for extreme decreases on the global and continental scale. In a model environment, it can be analyzed whether GPP extremes translate into changes in the net carbon uptake. Hence, in this study, we investigate how extremes in climate and the carbon cycle are related in current Terrestrial Biosphere Models (TBMs). In particular, we work with a suite of 10 state-of-the-art TBMs from the North American Carbon Program (NACP) Multi-scale Synthesis and Terrestrial Model Intercomparison Project (MsTMIP) described in *Huntzinger et al.* [2013] and *Wei et al.* [2013].

While simulated outputs are not direct observations of the carbon cycle, they integrate our current understanding of carbon exchanges between terrestrial ecosystems and the atmosphere, and therefore are a useful tool for several reasons. First, simple plausibility checks of the relationships found in the models can confirm model performance or foster reevaluation of specific model mechanisms. Second, analyzing model agreement can identify individual models that stand out against the rest. This can be useful if one can trace back the specific mechanisms that make a model an outlier in a particular situation, especially because some models that participated in MsTMIP are also used in coupled and/or offline projections of future carbon uptake. Third, due to the framework of MsTMIP [*Huntzinger et al.*, 2013], specific differences in the model output can be attributed to differences in intrinsic model structural characteristics, parameters, and initial states. Finally, model results can yield novel hypotheses based on our current understanding of the processes at work. While we cannot address each of the above points in full detail in this study, we provide first results about how MsMTIP models behave during large-scale extreme events. Results from this study can then later be evaluated against observations, e.g., from carbon flux data obtained by eddy-covariance flux towers (compiled in FLUXNET) [*Baldocchi et al.*, 2001; *Baldocchi*, 2008].

In this contribution, we analyze how current carbon cycle models translate extreme events in climate variables into (possibly extreme) responses in carbon fluxes. We address this question by looking from both driver and impact perspectives [*Smith*, 2011]. More specifically, we first identify temperature (T) and precipitation (P) extremes and estimate their immediate impact on the terrestrial carbon fluxes. Some extremes in temperature and precipitation can be strongly coupled, for instance, heat extremes and droughts [*Mueller and Seneviratne*, 2012]. We will therefore discuss whether the impact of a compound event (T and P simultaneously extreme) exceeds the expected additive impact (sum of impacts when either T or P is extreme). Besides their immediate impact, climate extremes can have strong lagged impacts on terrestrial carbon fluxes [*Reichstein et al.*, 2013]. Warm seasons can enhance heterotrophic respiration in grasslands a year later, soil frost can increase sensitivity of heterotrophic respiration of forests to summer drought and tree mortality can increase after severe droughts [*Reichstein et al.*, 2013]. Such lagged and legacy effects of extreme climate events, however, are still poorly understood [*McDowell*, 2011] and thus rarely correctly implemented in current carbon cycle models. Thus, we also analyze whether climate extremes cause large-scale lagged impacts.

Droughts and heat waves, as well as wind throw, fires, and insect infestation can trigger strong alterations in GPP and/or TR [*Reichstein et al.*, 2013], but not all extreme changes in terrestrial carbon fluxes need to be

Table 1. MsTMIP Terrestrial Biosphere Models (TBMs) Used in This Study Including Model Run (BG1 and SG3 Are the Best Estimates From the Global Runs, Models That Have BG1 Include a Nitrogen Cycle), Model Output Version (Internal MsTMIP Versioning), References, and C Fluxes That Are Included in Defining NEE[a]

Model	Run	Run Version	Reference	NEE Includes
Biome-BGC[b]	BG1	v2	*Thornton et al.* [2002]	fire emissions
CLM4[c]	BG1	v1	*Shi et al.* [2011] and *Mao et al.* [2012]	fire emissions, land use change, product decay,
CLM4VIC[d]	BG1	v1	*Li et al.* [2011]	maintenance respiration deficit
DLEM[e]	BG1	v3	*Tian et al.* [2011, 2012]	land use change, product decay
GTEC[f]	SG3	v2	*Ricciuto et al.* [2011]	product decay
ISAM[g]	BG1	v3	*Jain et al.* [1996]	land use change
LPJ-wsl[h]	SG3	v3	*Sitch et al.* [2003]	fire emissions, land use change
ORCHIDEE-LSCE[i]	SG3	v3	*Krinner et al.* [2005]	land use change, product decay
VEGAS[j]	SG3	v2.2	*Zeng et al.* [2005]	fire emissions, land use change, product decay
VISIT[k]	SG3	v3.1	*Ito and Inatomi* [2012]	

[a]Best estimates in MsTMIP always include annually changing land use cover as a driver. Hence, land use change only appears in the last column if a model additionally tracks emissions from land use and land cover changes.
[b]BIOME-BGC = Global Biome Model-Biogeochemical Cycle.
[c]CLM4 = Community Land Model.
[d]CLM4VIC = CLM with Variable Infiltration Capacity.
[e]DLEM = Dynamic Land Ecosystem Model.
[f]GTEC = Global Terrestrial Ecosystem Carbon model.
[g]ISAM = Integrated Science Assessment Model.
[h]LPJ-wsl = based on the Lund–Potsdam–Jena managed Land (LPJmL) model.
[i]ORCHIDEE = Organising Carbon and Hydrology In Dynamic Ecosystems.
[j]VEGAS = Vegetation Global Atmosphere and Soil.
[k]VISIT = Vegetation Integrative SImulator for Trace gases.

driven by extreme drivers [*Handmer et al.*, 2012]. Hence, in a second assessment, we identify extremes in C fluxes and analyze the concurrent climate conditions. More specifically, using driver data of MsTMIP, we investigate the concurrent state of *T* and *P* during C flux extremes.

Ecosystems in different regions are limited by different environmental factors. Cold temperatures often limit growth in boreal and temperate regions, whereas in tropical areas it is often warm enough but growth can be limited by water availability or cloud cover [*Nemani et al.*, 2003]. Tropical forests also operate close to their optimal photosynthesis temperature, however, and could be impacted by hot temperatures [*Clark*, 2004; *Corlett*, 2011]. In fact, the interannual correlation between (tropical) CO_2 anomalies and temperature anomalies is larger than with precipitation anomalies [see, e.g., *Wang et al.*, 2013]. To investigate whether different ecosystems react differently to extreme climate conditions, we compare C flux responses to extreme conditions of *T* and *P* between tropical, temperate, and boreal forests.

2. Material and Methods

2.1. MsTMIP

We use a suite of models from the North American Carbon Program (NACP) Multi-scale Synthesis and Terrestrial Model Intercomparison Project (MsTMIP) described in *Huntzinger et al.* [2013] and *Wei et al.* [2013]. The model simulations all follow the same experimental design and, more importantly, are all driven with the same set of climate drivers. This setting allows for an investigation of modeled impacts of climate extremes across a variety of different C cycle models. For this study, we use the global runs with "everything turned on," meaning that models are driven with time-varying climate and atmospheric CO_2 concentrations, land use and land-cover change (SG3), and nitrogen deposition (BG1; note that not all models include a nitrogen cycle). In the framework of MsTMIP, these runs are the "best estimates" of C fluxes submitted by the modeling teams. We use the 10 models shown in Table 1.

We restrict ourselves to temperature (*T*) and precipitation (*P*) as climatic drivers. For C fluxes we use GPP, total respiration (TR), and net ecosystem exchange (NEE). TR is defined as the sum of autotrophic and heterotrophic respiration. NEE is the sum of TR, disturbance fluxes (e.g., fire), product emissions, and aquatic fluxes, minus GPP [*Huntzinger et al.*, 2013]. By including disturbances, product emissions and aquatic C fluxes, the definition of NEE used in MsTMIP follows the recommendations of *Hayes and Turner* [2012] [see also *Chapin et al.*, 2006]. Depending on the model architecture, the factors included in NEE differ between

models (Table 1). We use the following sign conventions for GPP, TR, and NEE. GPP is always positive and describes a C flux from the atmosphere to the biosphere. TR is always positive and describes a C flux from the biosphere to the atmosphere. Positive NEE means a C release from the biosphere to the atmosphere, and vice versa. In this study we focus on the last 30 years (1981–2010), although MsTMIP output data are available for the period 1901–2010. We choose this period because, first, 30 years is the common time span to define climate reference periods (according to the World Meteorological Organization) [*Burroughs*, 2003] and second, because in this time span, environmental drivers are well constrained by observations. To assess changes in C fluxes relative to the long-term mean, prior to any further analysis, we subtract the linear trend of the time series of GPP, TR, and NEE at each location and subsequently subtract the average seasonal cycle of the years 1981–2010. We also linearly detrend T at each location. Throughout the paper, we call a point in a three-dimensional data cube (latitude × longitude × time) a *voxel* (short for volumetric pixel, used, e.g., in Neuroscience or computer gaming).

2.2. Climate Extremes

We focus on the impacts of T and P extremes. To identify extremes in P we rely on the standardized precipitation index (SPI) [*McKee et al.*, 1993], which is widely used to assess droughts [e.g., *Lloyd-Hughes*, 2012] and to study land-atmosphere interactions [*Mueller and Seneviratne*, 2012; *Holmgren et al.*, 2013]. The SPI is calculated for each month and location based on monthly precipitation data, which are typically well approximated by a gamma distribution. As in the standard approach, monthly precipitation time series are fitted to a gamma distribution to obtain a probability density function of precipitation [*McKee et al.*, 1993]. This distribution is then transformed to a standard normal distribution. The mean SPI value for the reference period is thus zero. Positive (negative) values hence signify higher (lower) than average precipitation. SPI is also frequently used as a proxy for soil moisture [*Seneviratne et al.*, 2010; *Mueller and Seneviratne*, 2012] and compares well with more sophisticated meteorological drought indicators [*Joetzjer et al.*, 2013].

To be able to compare time series of T at different locations and to make T and P extremes comparable, we define the *standardized temperature index* (STI) in the spirit of the SPI. Because T anomalies can be assumed to be normally distributed [see, e.g., *Hansen et al.*, 2012], however, we omit fitting a gamma distribution and directly fit a standard normal distribution to each detrended monthly temperature time series.

For P we use a time scale of 3 months which is a common choice in drought assessments [*Mueller and Seneviratne*, 2012; *Lloyd-Hughes*, 2012]. Hence, before fitting a gamma distribution, each P value is replaced by the average over the current and the two preceding P values. Time scales of 6, 12, and 24 months are also common for analyzing long-lasting droughts [*McKee et al.*, 1993]. For T extremes, on the other hand, we consider the instantaneous response of terrestrial carbon fluxes most relevant due to the immediate decrease in photosynthetic activity of plants in response to extreme temperatures [*Berry and Bjorkman*, 1980]. Hence, for T, we choose a time scale of 1 month.

To identify extremes we set a threshold of 2, which is, in the case of SPI, associated with extreme drought [*McKee et al.*, 1993] and a commonly used threshold [*Lloyd-Hughes*, 2012]. This corresponds to approximately the 2.3% highest and lowest SPI and STI. We thus consider four different categories of climate extreme events: (1) *drought*: SPI < -2 ($-P$), (2) *extremely wet period*: SPI > 2 ($+P$), (3) *cold spell*: STI < -2 ($-T$), and (4) *heat extreme*: STI > 2 ($+T$).

The identifiers in parentheses are used in figures throughout the paper.

2.3. Extremes in Carbon Fluxes

To identify extremes in GPP, TR, and NEE we use a definition that mimics the statistical properties of SPI. Let X be a time series of a certain month across all years in the record, we define $x \in X$ as extreme if

$$|x - \bar{X}| > k\sigma(X) \tag{1}$$

where $\bar{X}$ and $\sigma(X)$ are the empirical mean and standard deviation of X, respectively. We choose $k = 2$ here to obtain a similar degree of extremeness between carbon cycle and climate extremes. In fact, if C cycle anomalies are normally distributed, $k = 2$ corresponds to the criterion used to identify climate extremes. Tests using $k = 1.8$ and $k = 2.2$ confirmed that our conclusions remain consistent for a less strict and a stricter definition of extreme conditions, respectively. Similarly, our conclusions are not sensitive to the choice of time scales for SPI and STI.

2.4. Aggregation

For most of our analyses, we aggregate point extremes to spatiotemporal extreme *events*. We use the aggregation scheme initially suggested for droughts by *Lloyd-Hughes* [2012] and further elaborated for the case of Earth observation data by *Zscheischler et al.* [2013]. Individual voxels that are extreme are joined if they are adjacent in space or in time to form three-dimensional extreme events. The newly formed events can then be ordered according to their spatial extent or their overall impact, i.e., their integrated deviation from "normal" conditions (normal here refers to the averaged seasonal cycle). Throughout this paper we will sort extreme events according to their overall impact. The *size* of an extreme event is thus given as the integral of the SPI, STI, or C flux anomalies over the spatiotemporal extent of that event.

2.5. Attribution

For the *forward* assessment we compute the impact of extreme climate events by integrating carbon cycle flux anomalies (GPP, TR, and NEE) over the spatiotemporal domain of an extreme event in T or P. We calculate the cumulative impact of extreme climate events by adding the impacts of the n largest events.

We further propose a simple scheme to detect large-scale lagged impacts of extreme climate events. The temporal extent and shape of climate extremes can confound small-scale lagged impacts. Moreover, the differences in C flux sensitivity across models further impede a straightforward assessment of lagged effects. Because a detailed analysis of various small-scale lagged impacts of climate extremes is beyond the scope of this study, here we suggest an approach to detect lagged impacts of a magnitude that dominates both the shape of extreme events and the model sensitivity.

To determine whether a climate extreme has a lagged impact on C fluxes, we first integrate the C flux anomalies over the spatiotemporal extent of the climate extreme event itself. We then integrate the C flux anomalies over an equivalent spatiotemporal extent, but shifted by 1 to 12 months backward in time relative to the span of the actual climate extreme. Finally, we repeat the same analysis, but shifting the spatiotemporal extent 1 to 12 months forward in time. The resulting integrated C flux anomalies (Figure 6) therefore represent the C flux anomalies over periods that extend before (after) the start (end) of the climate anomaly. Because the actual climate extremes extend over more than a single month, the C flux anomalies are nonzero even when looking at spatiotemporal extents shifted backward in time. Any asymmetry between the impact of shifts backward in time (due only to the fact that the extreme climate events have a greater than 1 month duration) and the impact of shifts forward in time (due not only to the fact that the extreme climate events have a greater than 1 month duration, but also to any lagged effects of these climate extremes on C fluxes), is therefore a qualitative measure of the lagged effects of various types of climate extremes on C fluxes.

In the spirit of the forward assessment, for our *backward* assessment, we compute the mean SPI and STI over the spatiotemporal domain spanned by an extreme event in GPP, TR, or NEE as diagnosed from each model's output. For each C flux extreme event we can then draw a point onto the two-dimensional plane spanned by SPI and STI. To visualize climate conditions during C flux extremes, we fit a bivariate Gaussian distribution to the points generated in this manner where we use the 100 largest C flux events. We then plot the contour line of the first standard deviation for each model or region.

2.6. Carbon Flux Sensitivity to Climate Extremes

We investigate modeled flux sensitivity to compound extreme events (T and P extreme simultaneously). To do so, we divide the mean anomaly of GPP (TR, NEE) over each of the four conditions hot and dry (STI > 2, SPI < −2), hot and wet (STI > 2, SPI > 2), cold and dry (STI < −2, SPI < −2), cold and wet (STI < −2, SPI > 2) by the mean SPI and mean STI over the same voxels. The resulting unit measures the change of C flux per unit SPI per unit STI and gives us an idea about the general sensitivity of C fluxes to climate extremes. For example, for dry and hot extremes we compute

$$\mathrm{Sens}^{-2,2} = \frac{\overline{x}_{\mathrm{SPI}<-2,\mathrm{STI}>2}}{|\overline{\mathrm{SPI}}_{\mathrm{SPI}<-2,\mathrm{STI}>2}\overline{\mathrm{STI}}_{\mathrm{SPI}<-2,\mathrm{STI}>2}|}, \quad (2)$$

where x are C flux anomalies (GPP, TR, or NEE).

2.7. Compound Impact Versus Additive Impact

Compound events are defined as "(1) two or more extreme events occurring simultaneously or successively, (2) combinations of extreme events with underlying conditions that amplify the impact of the events, or

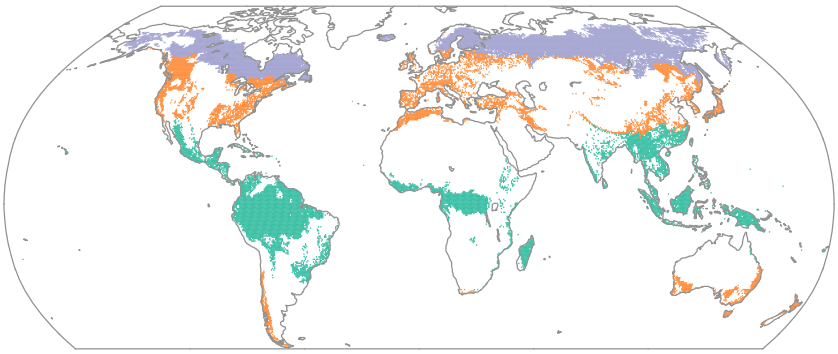

Figure 1. Forest biomes used for regional analysis, including tropical forests (green), temperate forests (orange), and boreal forests (purple).

(3) combinations of events that are not themselves extremes but lead to an extreme event or impact when combined" [*Seneviratne et al.*, 2012; see also *Leonard et al.*, 2013]. In the framework of MsTMIP, we make an attempt to quantify the effects of (2) and (3). As *compound* extreme we define voxels where *T* and *P* are simultaneously extreme and call their impact a compound impact. The *additive* impact is the impact of extremes in *T* plus the impact of extremes in *P* (also includes the compound events). To estimate the difference between compound and additive impacts, we plot the compound against the additive impact for each model (10), each flux (GPP, TR, and NEE), and each extreme climate condition (hot and dry, hot and wet, cold and wet, cold and dry). The distance to the 1:1 line is a measure of the difference between the compound impact and the additive impact.

2.8. Regional Analysis

We compute sensitivities according to equation (2) but only for one climate variable (*T* or *P*) in tropical, temperate, and boreal forests (Figure 1). We further conduct the backward assessment (section 2.5) on these three regions to analyze whether the climatic conditions leading to extreme C flux responses differ across biomes.

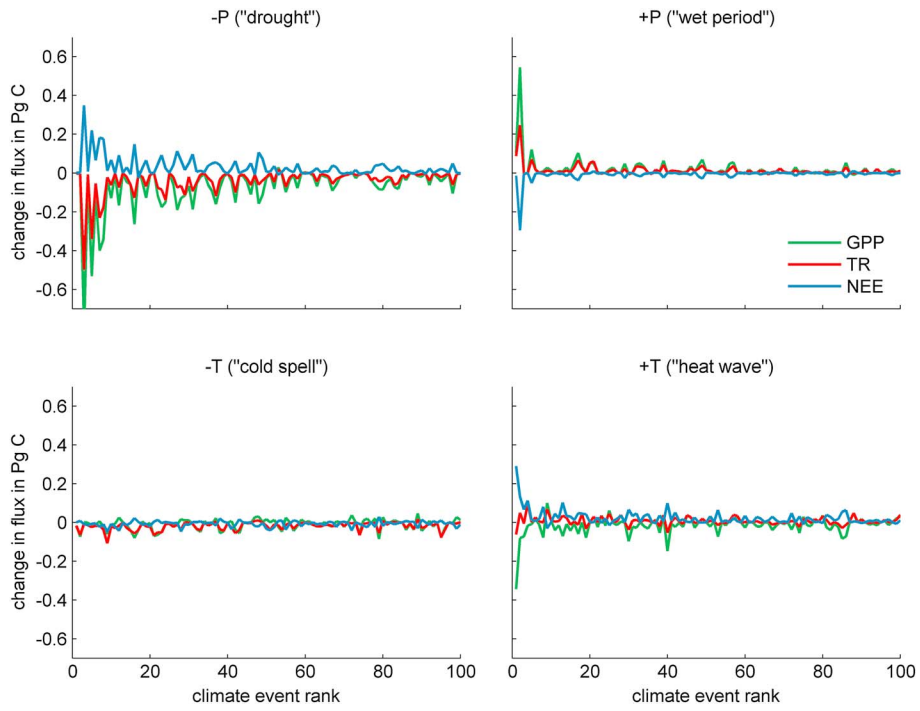

Figure 2. Impact of the 100 largest extreme events in (top) precipitation (*P*) and (bottom) temperature (*T*) on the carbon fluxes GPP (green), TR (red), and NEE (blue), shown as an average across the 10 examined models.

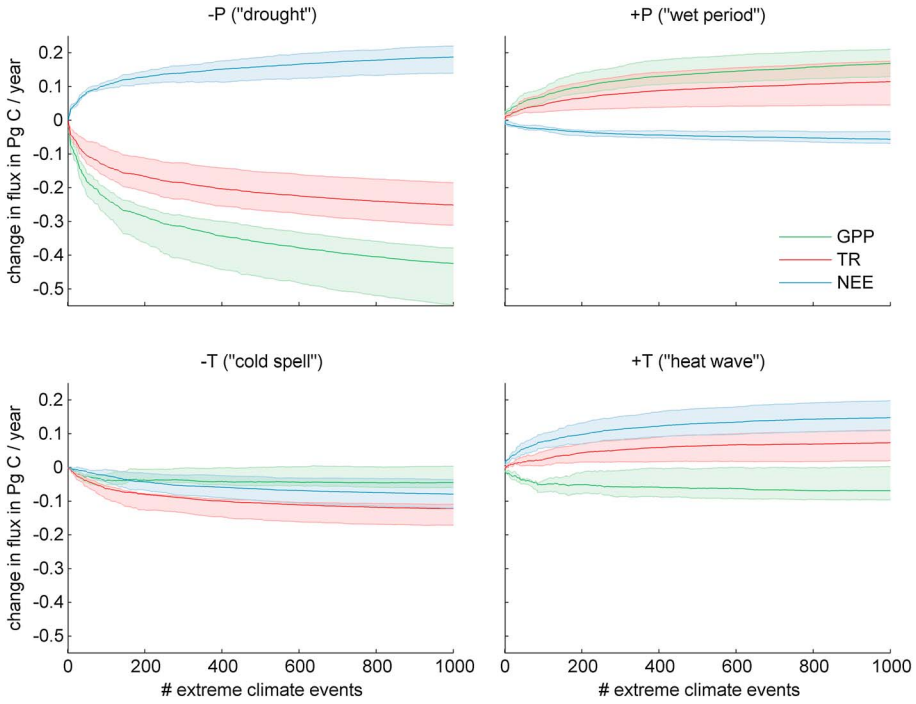

Figure 3. Cumulative impact of the 1000 largest extremes in (top) precipitation (*P*) and (bottom) temperature (*T*) on GPP (green), TR (red), and NEE (blue). Climate extreme impacts are averaged over the whole study period (1981–2010). Shown are the model averages and the model interquartile range (spread over five models, shaded areas).

3. Results

3.1. Forward Assessment

This section deals with extreme events computed at the global scale. For extremes at biome scale refer to section 3.3.

3.1.1. Impacts of Large Extreme Climate Events

Overall, droughts lead to the strongest responses in the carbon fluxes (−*P* in Figure 2). GPP strongly decreases in response to drought. The concurrent smaller decrease in TR partly compensates the effect of GPP, resulting in an anomalous increase in NEE of up to 0.19 ± 0.06 Pg C/yr (model mean ± standard deviation) for the 1000 largest −*P* extremes (Figure 3). Droughts, hence, promote net carbon release to the atmosphere or a decrease in C sink. Wet periods show the opposite behavior, although much less pronounced. Temperature extremes yield a less clear C flux signal (Figure 2), but the cumulative impact of heat extremes tends to reduce GPP and increase TR. This compounding effect results in an increase in NEE comparable to that of droughts (0.15 ± 0.05 Pg C/yr, Figure 3). While the carbon flux response to climate extremes tends to point in the same direction for most models, model spread is relatively large.

3.1.2. C Flux Sensitivity to Compound Extreme Extremes

The way in which modeled carbon fluxes respond to varying climate conditions largely differs across models. Figure 4 shows the sensitivities of C fluxes for all 10 models for the four compound extreme conditions hot and dry (STI > 2, SPI < −2), hot and wet (STI > 2, SPI > 2), cold and wet (STI < −2, SPI > 2), and cold and dry (STI < −2, SPI < −2) for GPP, TR, and NEE. Models are sorted according to the impact of hot and dry extremes on NEE (Figure 4i). The model LPJ-wsl is most sensitive to this condition and also shows the largest response for most of the other variables and conditions. At the other end of the spectrum, VEGAS shows the smallest response of NEE to hot and dry extremes, but it is close to the model average in terms of its sensitivity of GPP and TR. Further analyses showed that the relative sensitivity of each model to different types of extremes is mostly consistent, i.e., C fluxes are generally more sensitive to changes in *T* and *P* in some models and less sensitive in others.

3.1.3. Compound Versus Additive Impact

Model responses to extreme climate conditions largely agree on whether or not the impact of compound extremes exceeds their additive impact (i.e., in Figure 5, points lie mostly on the same side of the 1:1 line), though responses differ substantially in magnitude. The impact of drought *and* extreme heat (SPI < −2 and

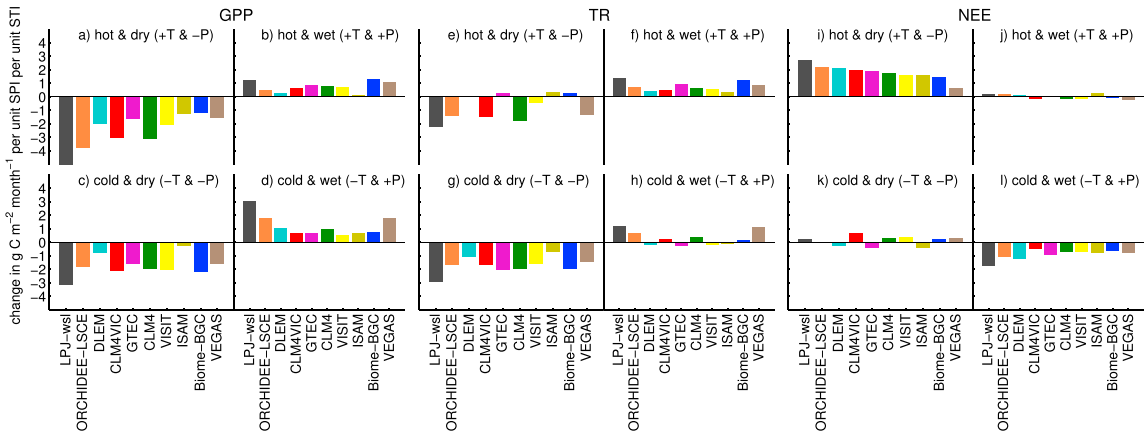

Figure 4. Sensitivity of modeled C fluxes to compound climate extremes. Models are sorted according to their NEE response to hot and dry.

STI > 2) on GPP, TR, and NEE exceeds the sum of the individual impacts by 5.2 ± 2.7, 2.3 ± 1.6, and 2.9 ± 1.1 g C m^{-2} per month, respectively (Figures 5a, 5e, and 5i). Both the compound impacts of cold *and* wet as well as cold *and* dry conditions on GPP are similar to the sum of the individual impacts (Figures 5b and 5c). The positive effects of cold *and* wet periods on NEE exceed the expected effect from the sum of impacts of cold *or* wet conditions (Figure 5l).

3.1.4. Time Lags

As expected, the cumulative impact over the 1000 largest climate extreme events peaks when the corresponding C flux anomalies are integrated over the spatiotemporal extent of the climate extreme itself, indicating that the largest C flux impacts are experienced during the extreme climate events themselves (Figure 6).

Because extremes in *P* last longer than extremes in *T*, the impact of *P* extremes on C fluxes is observed even when the spatiotemporal extent over which C fluxes are integrated is shifted by several months either forward or backward in time. Most noteworthy, however, is any asymmetry in the integrated C flux anomalies when the spatiotemporal extent is shifted forward versus backward in time relative to the extent of the actual *P* extremes. The C flux anomalies persisting for longer positive time shifts relative to negative time shifts for *P* extremes indicates a lagged impact of *P* extremes on C fluxes. This is especially evident for positive precipitation extremes (Figure 6, top right).

3.2. Backward Assessment

At the global scale, extreme events in GPP and TR are more closely associated with changes in water availability (SPI) relative to changes in temperature (STI; Figure 7, contour lines are shifted more along the

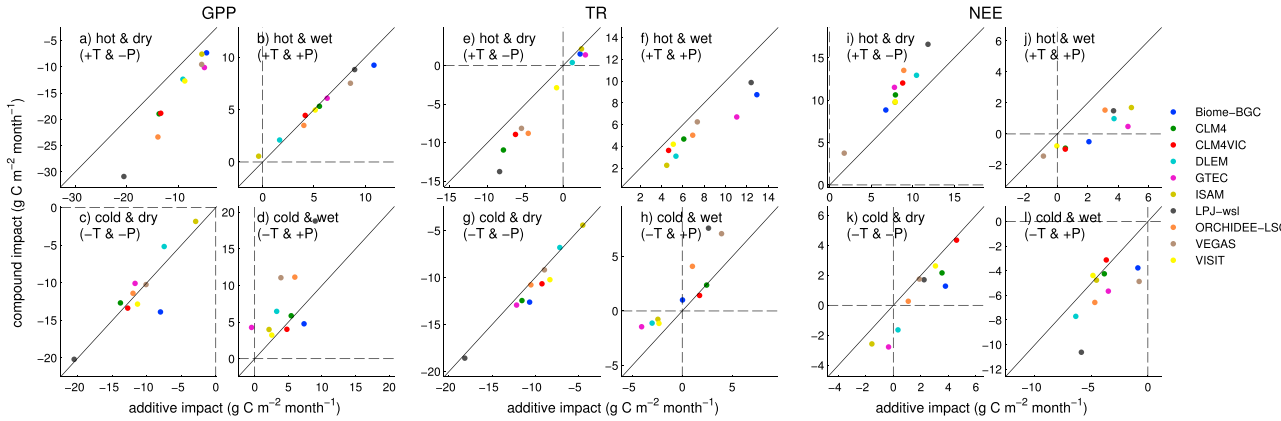

Figure 5. Impacts of compound climate extremes versus additive impact of *P* and *T* extremes. Shown is the response of GPP, TR, and NEE of all 10 models to the four compound extreme climate conditions hot and dry, hot and wet, cold and wet, and cold and dry.

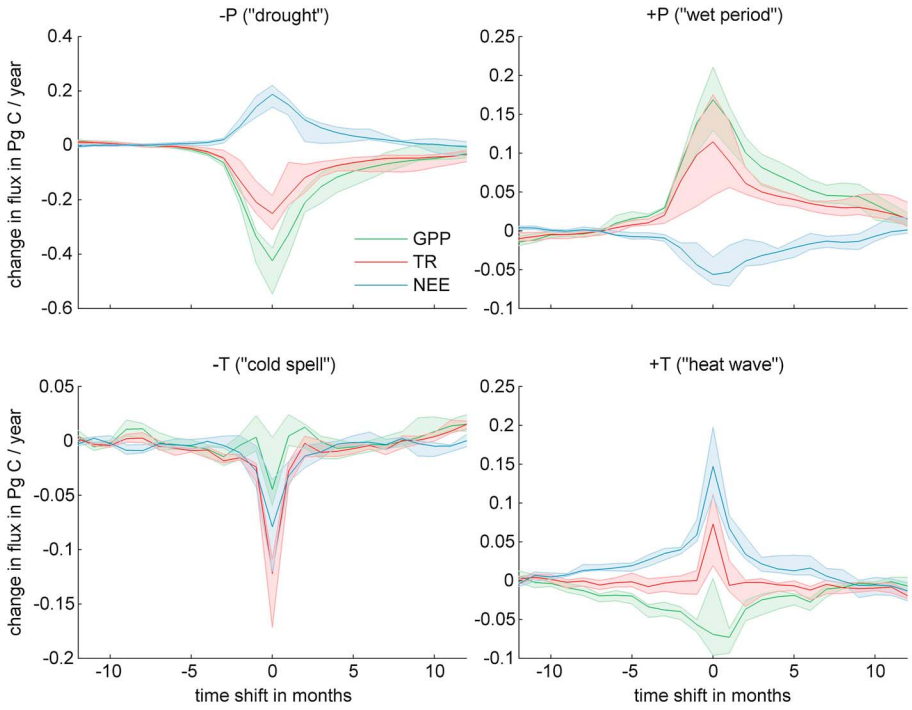

Figure 6. Lagged impacts of the 1000 largest extreme events in (top) precipitation (*P*) and (bottom) temperature (*T*) on GPP (green), TR (red), and NEE (blue). Carbon fluxes are integrated over the spatiotemporal extent of extreme climate events shifted in time by up to 12 months before, relative to the events themselves and up to 12 months after. Shown are the model averages and their interquartile range (spread over five models, shaded areas).

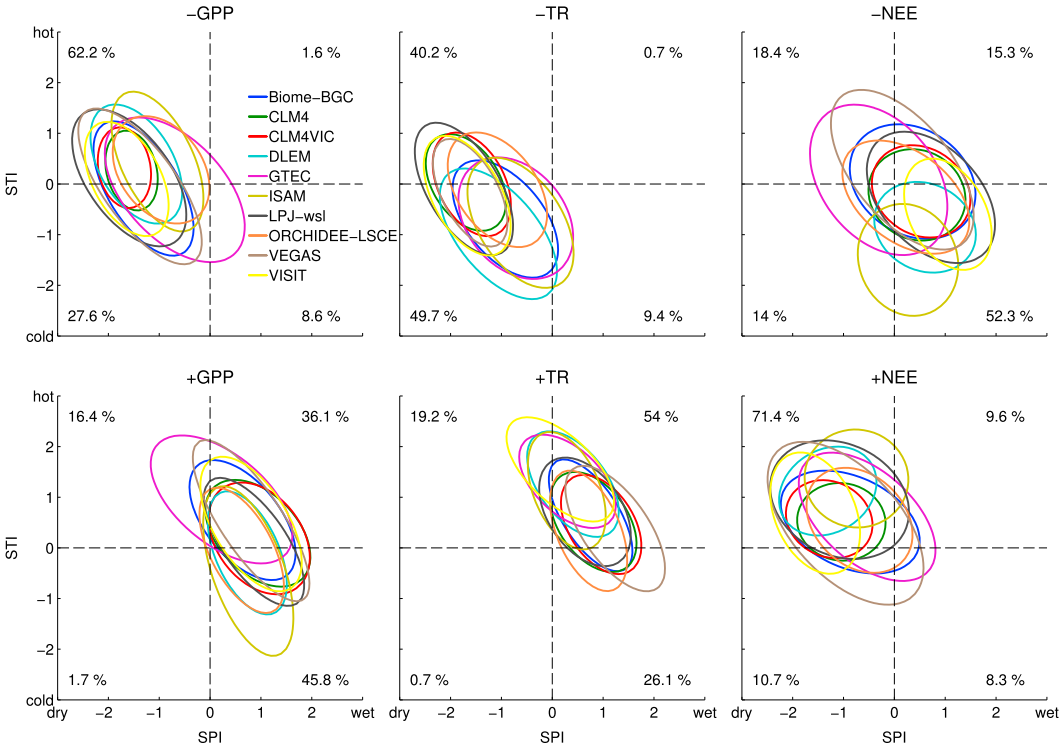

Figure 7. Climatic conditions (*T* and *P*) during extremes in carbon fluxes. Ellipses depict contour lines of 1 standard deviation of bivariate Gaussian distributions fitted to the SPI/STI values averaged over the spatiotemporal domain of each of the 100 largest positive (+) and negative (−) extreme events in GPP, TR, and NEE, for each model. Percentages in the corners show the fraction of events falling in the respective quadrant across all models.

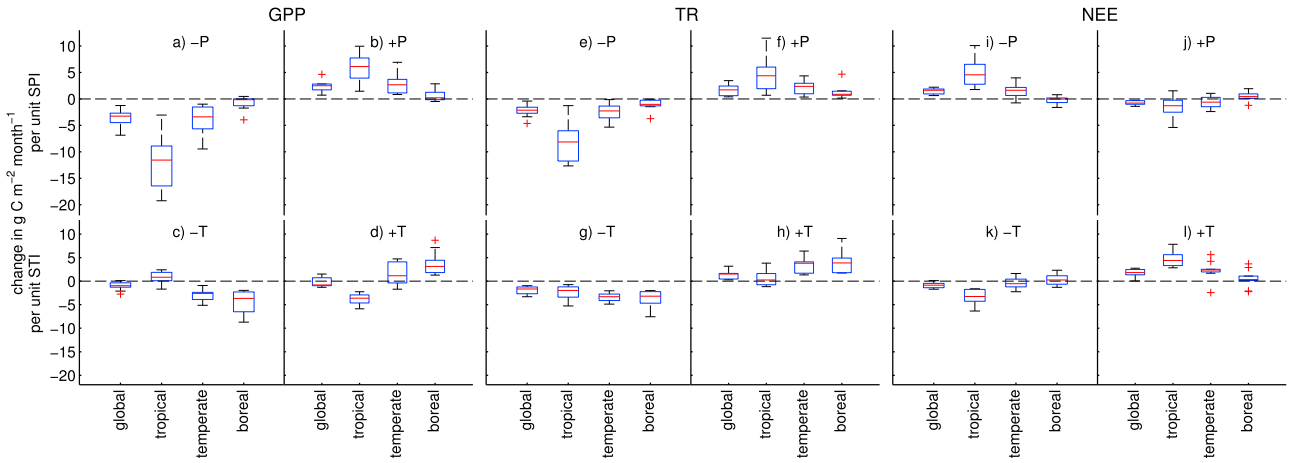

Figure 8. Sensitivity of C fluxes to extreme climate conditions globally and in tropical, temperate, and boreal forests. Boxplots depict the spread in the GPP, TR, and NEE response to dry, wet, hot, and cold conditions across all 10 models.

moisture axis than along the temperature axis). Negative extremes in GPP coincide with dry conditions in all models (Figure 7). This is also true for negative extremes in TR. Dry conditions also accompany negative extreme events in the gross fluxes (GPP and TR) more often (89.8% and 89.9%) than wet conditions accompany positive extremes (81.9% and 80.1%, respectively). Positive extreme events in NEE (net carbon release to the atmosphere or decrease of carbon sink) are most often associated with dry and hot conditions (71.4%). The fraction of negative extreme events in NEE associated with the opposite climate conditions,

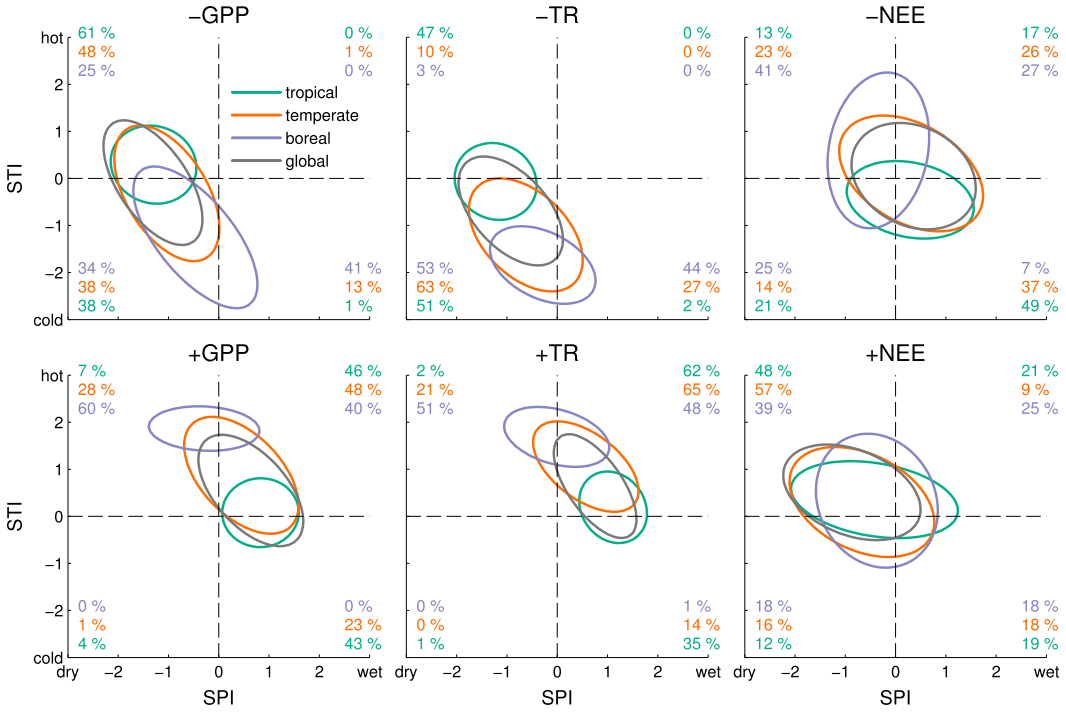

Figure 9. Similar to Figure 7. Here Gaussian distributions are fitted to SPI/STI values averaged over the spatiotemporal domain of each of the 100 largest positive, + (negative, –) extreme events in GPP (TR, NEE) in each of the 10 models. The contours represent the temperature and precipitation conditions across the resulting 1000 events (i.e., 10 models × 100 events). Extreme events are computed on the globe (gray), tropical forests (green), temperate forests (orange), and boreal forests (purple), using the division of Figure 1. Percentages in the corners show the fraction of events falling in the respective quadrant for each region separately.

cold and wet, is much lower (52.3%). Overall, model spread is largest for negative extremes in NEE (i.e., increased uptake or decreased source; Figure 7, top right).

3.3. Regional Assessment

C fluxes in tropical forests show a strong response to extremes in water availability. In contrast, in boreal forests C fluxes respond more strongly to extremes in temperature (Figure 8). The C flux response in temperate forests always lies between those of boreal and tropical forests. Models mostly agree in sign in their C flux response to extreme climate conditions. Model spread is particularly high for the GPP and TR response to heat extremes in the boreal forests, leading to a highly uncertain NEE response ranging from −2.2 (GTEC) to 3.7 (LPJ-wsl) g C m^{-2} $month^{-1}$ (Figures 8d, 8h, and 8l). There was no relationship between process inclusion of fire emissions and NEE response. Note that C fluxes in boreal regions are generally much smaller compared to the tropics; hence, we also expect a smaller change during extreme climate conditions.

Negative extremes in GPP and TR are mainly associated with dry conditions in tropical forests but with cold conditions in boreal forests (Figure 9). Positive extremes in NEE are associated with dry and hot conditions in tropical forests, whereas in boreal forests there is no clear trend visible. For boreal forests also, NEE extremes can be accompanied by largely differing environmental conditions (Figure 9, area in contour line larger). Temperate forests are always located in between tropical and boreal forests (Figure 9).

4. Discussion

4.1. Forward and Backward Assessment

Drought and heat extremes in MsTMIP simulations differ in their impacts on GPP and TR, which shape their impact on NEE. Drought reduces both GPP and TR. This is consistent with observational studies [*Law et al.*, 2001; *Ciais et al.*, 2005; *Meir et al.*, 2008; *Schwalm et al.*, 2010, 2012]. The impact of heat stress on GPP depends on whether the ecosystem in question is temperature limited [*Nemani et al.*, 2003; see also section 3.3] but tends to reduce GPP at the global scale. TR, on the other hand, increases with higher temperatures, which is in agreement with observations [*Rustad et al.*, 2001; *Zhao and Running*, 2010; *Mahecha et al.*, 2010; *Anderson-Teixeira et al.*, 2011]. Models mostly agree in the direction of their response to extreme climate conditions, but the absolute magnitude of the response differs greatly, in particular, for GPP and TR. Differences in model mechanisms probably contribute to this spread, although it is hard to draw general conclusions solely from whether a model includes a particular characteristic or not [*Huntzinger et al.*, 2013, Tables S1–S4]. Sensitivity analyses of model parameters would probably help to explain the model spread. Moreover, the MsTMIP protocol includes model runs with reduced complexity (e.g., no land use and land cover change, constant CO_2). If a similar analysis on these runs would show a smaller model spread one could narrow down the mechanisms responsible for the large model spread observed here.

Although the anomalies in GPP and TR caused by climate extremes may seem small compared to the respective global values of 128 $\pm$ 28 and 121 $\pm$ 26 Pg C/yr (model mean $\pm$ standard deviation), these numbers are averaged over the whole study period such that the maximum impact in a given year may be much larger. Moreover, the main interest here lies in NEE, and GPP and TR anomalies can translate into an NEE anomaly with a much higher relative impact. In fact, an average increase of about 0.19 and 0.15 Pg C/yr in NEE (droughts and heat waves, respectively) is substantial, given that global NEE is around 2.3 $\pm$ 2.6 Pg C/yr (estimates of the residual land sink lie around 2.3 Pg C/yr, averaged over the same time period) [*Le Quéré et al.*, 2013].

Despite a relatively large model spread in the gross fluxes GPP and TR in response to extreme climate events, model agreement for the NEE response at global scale is relatively high. This behavior has been observed before [*Huntzinger et al.*, 2012; *Raczka et al.*, 2013]. Models can produce plausible values for NEE even if they overestimate (or underestimate) GPP and heterotrophic respiration, for instance, if they are "tuned" to flux tower observations of net ecosystem productivity [*Mahecha et al.*, 2010; *Huntzinger et al.*, 2012].

A metaanalysis of manipulated ecosystem experiments with higher *T* and altered *P* demonstrated that warming increases both photosynthesis and respiration but showed no significant effects on net C uptake [*Wu et al.*, 2011]. Most of the experiments were performed in temperate and boreal regions where systems are temperature limited. The MsTMIP model results from temperate and boreal forests agree well with these findings (Figure 8). *Wu et al.* [2011] also found that decreased *P* suppressed soil respiration, ecosystem photosynthesis, and net C uptake, whereas increased *P* stimulated respiration, ecosystem photosynthesis, and net C uptake. This is also in accordance with MsTMIP results.

Our analysis of compound extremes showed that, for heat waves and droughts in particular, their combined impact is larger than the sum of their individual impacts. The metaanalysis of *Wu et al.* [2011] showed that the combined effect of elevated *T* and alterations in *P* tends to be smaller than expected from the single-factor responses. However, because their analysis mainly focused on temperate and boreal areas and temperatures were elevated and not extreme, *T* might rather exhibit a compensatory effect in the interaction with decreases in precipitation.

In the backward assessment, as in the forward assessment, the negative effects of drought and extreme heat on NEE are more apparent than the positive effects of excessive water availability and colder temperatures. In particular, we observe a large model spread for the attribution of negative extremes in NEE (abnormal C sink or decrease in C source) to specific climate conditions. This might be a result of Liebig's law of the Minimum [*von Liebig*, 1847] or similar formulations of growth as a function of limited resources, which are implemented in most TBMs [*Rastetter*, 2011]. According to such a formulation of limiting factors, to achieve a net carbon uptake (and ultimately growth) that is abnormally high, a number of accompanying factors have to be optimal, whereas drought or extreme heat alone can suffice to reduce growth drastically. Negative extremes in NEE also directly affect soil organic carbon (SOC), whereas positive extremes are first the result of increases in GPP, and then through time this can increase SOC and wood pools. Consequently, the larger disagreement between the models about the environmental conditions favoring excessive growth might reflect their different treatments of limiting factors.

The forward and backward assessments provide a complementary picture on impacts of climate extremes and possible causes of extremes in carbon fluxes that is derived from our current understanding of the terrestrial carbon cycle. While droughts and heat waves decrease GPP, and wet periods increase GPP, negative (respectively positive) extremes in GPP are driven by dry (wet) conditions. In the forward analysis, droughts decrease GPP more than heat waves do. This is supported by the backward analysis where GPP extremes are associated more frequently with stronger deviations in water availability than with changes in temperature, which is in good agreement with recent studies about GPP extremes [*Zscheischler et al.*, 2014a, 2014b]. Moreover, the increase in GPP due to wetter or colder conditions is smaller than the decrease due to dryer or hotter conditions. This is mirrored in the backward analysis by a smaller deviation of *T* and *P* for positive GPP extremes compared to negative GPP extremes. For TR, all the above is also true, except that here heat extremes increase TR. Also, compared to GPP extremes, TR extremes are to a larger extent driven by deviations in *T*. Droughts and heat waves increase NEE similarly strongly, whereas cold temperatures and wet periods decrease NEE to a smaller degree. Again, in the backward analysis the attribution of positive NEE extremes to hot and dry conditions supports the findings from the forward analysis. Accordingly, the shift toward wet and cold conditions for negative extremes is less pronounced.

Overall, both perspectives (forward and backward) show that the relationship between droughts and heat waves with increasing NEE (abnormal C source or decrease in C sink) is stronger than the link between colder or wetter periods and decreases in NEE (abnormal C sink or decrease in C source). This is also because for high temperatures, decreases in GPP and increases in TR compound each other, leading to a strong NEE response, whereas for wet periods the effect of increasing GPP is nearly offset by a similar increase in TR (Figure 3). This differential behavior of GPP and TR in response to different climate extremes can also explain the very weak relationship between GPP extremes and independent NEE estimates [*Zscheischler et al.*, 2014a].

At this point we would like to emphasize that most of our conclusions are drawn from the global mean behavior averaged across 10 models. In particular, cold and hot temperatures can have opposing effects on C fluxes, depending on the underlying ecosystem (see also section 3.3). This might also explain why at global-scale changes in C fluxes seem to be more tightly coupled to deviations in *P* than to deviations in *T*.

One might argue that the differences in how the models treat fire might be one reason for differing results, in particular for NEE. We repeated the analysis using NEP = GPP−TR instead of NEE. The differences between the results from NEE and NEP were very small, and model spread was not substantially reduced. We assume this is because most fires and other disturbances are small compared to the scale of extreme events we are looking at in this study and thus do not affect the results significantly.

4.2. Time Lags

The largest impact of climate extremes takes place during the climate extreme itself. Nevertheless, we observe a longer response of C fluxes to *P* extreme events compared to *T* extreme events, explainable by a combination of the longer duration of *P* events and the longer time scales that *P* controls soil moisture than the response of ecosystem processes to changes in *T*. Droughts and extremely wet periods last on average 4.8 and 3.6 months compared to 1.8 and 1.7 months for cold spells and heat extremes, respectively (maximal duration of each event averaged over the 1000 largest extreme events). We further detected a strong lagged response in C fluxes for positive *P* extreme events. This is possibly related to excessive (re-)growth triggered by high water availability. A slight asymmetry can also be seen in response to droughts (−*P*), potentially caused by lagged impacts of some of the events. However, instantaneous impacts from a few very long droughts cannot be ruled out. It is difficult to draw general conclusions from our simple analysis of lagged impacts due to the confounding effects of the model sensitivity and the shape of specific extreme events (in the 3-D latitude × longitude × time space). Yet it seems that, despite their longer temporal extent, *P* extremes have longer-lasting impacts compared to *T* extremes. While some processes responsible for long-term lag effects following climate extremes are known [e.g., *Anderegg et al.*, 2013; *Hartmann et al.*, 2013; *Reichstein et al.*, 2013], they are often not (yet) implemented into current TBMs [*McDowell*, 2011]. Thus, we expect the identified lagged impacts to be a lower bound for what is occurring in reality.

4.3. Regional Analysis

Our results showed that C fluxes in tropical forests are more sensitive to *P* anomalies, whereas C fluxes in boreal forests respond more strongly to extreme changes in temperature. This is supported by the backward assessment, where negative extremes in GPP and TR are mainly associated with dry conditions in tropical forests but with cold conditions in boreal forests. Due to the small temperature variability in the tropics, temperature regimes which could have a significant impact on C fluxes are rarely realized. Hence, by using our definition of extremes based on local time series, temperature extremes in the tropics can be very small. Regardless, our results are in good agreement with experimental studies suggesting that tropical forest might generally be more sensitive to changes in water availability than to changes in temperature [*Clark*, 2004; *Clark et al.*, 2010]. Particularly, droughts have been shown to largely impact tropical forest mortality [*Phillips et al.*, 2010] and carbon stocks [*Brando et al.*, 2008]. Yet, it is expected that ongoing climate change will soon push temperatures in the tropics beyond current variability [*Mora et al.*, 2013], thus generating heat extremes that have not been experienced before, with uncertain impacts on tropical forests [*Clark*, 2004; *Corlett*, 2011].

In contrast to the global analysis, our results showed high uncertainty in the NEE response to extremely hot conditions in boreal forests. Climate predictions in the arctic and boreal regions are highly uncertain [*Stroeve et al.*, 2012; *Schneider von Deimling et al.*, 2012]. The strength and timing of the carbon-climate feedback to global warming in permafrost regions, for instance, continue to pose challenges to researchers [*McGuire et al.*, 2009; *Schaefer et al.*, 2011; *Koven et al.*, 2011]. Here, in the framework of MsTMIP, the climatic forcing is equal for each model. Nevertheless, model response to warming strongly diverges in boreal forests. This suggests that uncertainties in carbon cycle predictions in boreal regions are not only due to an incomplete understanding of climate regimes but also driven by incomplete knowledge about the processes governing the carbon cycle in these areas.

5. Conclusions

We have presented an analysis of climate and C flux extremes using model output data from MsTMIP. The two perspectives used give complementary results that further the understanding of the relationships between extremes in drivers and extreme impacts, as they are implemented in current TBMs. At the global scale, droughts and heat waves lead to large temporary net carbon release or decrease in C sink (increase in NEE), while colder and wetter periods lead to a comparably smaller net carbon uptake or increase in C sink (decrease in NEE). The models largely agree in this behavior, although the magnitude of the responses differs greatly across models.

We demonstrated that compound extremely hot and dry conditions have a larger impact on C fluxes than one would expect from their individual impacts. Compound events in which not all driving variables are extreme but which lead to an extreme impact are increasingly the focus of impact analyses [*Leonard et al.*,

Acknowledgments
We thank Dominique Bachelet and Altaf Arain for helpful comments on the manuscript. Funding for the Multi-scale Synthesis and Terrestrial Model Intercomparison Project (MsTMIP; http://nacp.ornl.gov/MsTMIP.shtml) activity was provided through NASA ROSES grant NNX10AG01A. Data management support for preparing, documenting, and distributing model driver and output data was performed by the Modeling and Synthesis Thematic Data Center at Oak Ridge National Laboratory (ORNL; http://nacp.ornl.gov), with funding through NASA ROSES grant NNH10AN681. Finalized MsTMIP data products are archived at the ORNL DAAC (http://daac.ornl.gov). This is MsTMIP contribution 3. J.Z. is member of the International Max Planck Research School for Global Biogeochemical Cycles (IMPRS-gBGC) and acknowledges funding from the European Community's Seventh Framework Program (FP7 2007-2013) under the grant agreements 226701, 283080, and 238366. *Acknowledgments for specific MsTMIP participating models is as follows.* Biome-BGC code was provided by the Numerical Terradynamic Simulation Group at University of Montana. The computational facilities were provided by NASA Earth Exchange at NASA Ames Research Center. (CLM4 and GTEC) This research is supported in part by the U.S. Department of Energy (DOE), Office of Science, Biological and Environmental Research. Oak Ridge National Laboratory is managed by UT-BATTELLE for DOE under contract DE-AC05-00OR22725. (CLM4VIC) This research is supported in part by the U.S. Department of Energy (DOE), Office of Science, Biological and Environmental Research. CLM4VIC simulations were performed using the Environmental Molecular Sciences Laboratory (EMSL), a national scientific user facility sponsored by the DOE's Office of Biological and Environmental Research and located at Pacific Northwest National Laboratory. PNNL is operated for the U.S. DOE by BATTELLE Memorial Institute under contract DE-AC05-76RLO1830. The Dynamic Land Ecosystem Model (DLEM) developed in International Center for Climate and Global Change Research, Auburn University, has been supported by NASA Interdisciplinary Science Program (IDS), NASA Land Cover/Land Use Change Program (LULUC), NASA Terrestrial Ecology Program, NASA Atmospheric Composition Modeling and Analysis Program (ACMAP), NSF Dynamics of Coupled Natural-Human System Program (CNH), Decadal and Regional Climate Prediction using Earth System Models

2013]. Such analyses largely extend the space of possible causes for extreme impacts and call for new tools to analyze extremes as multivariate probability distributions.

The biome-dependent analysis revealed that C flux extremes in tropical forests are more strongly coupled to water availability whereas C flux extremes in boreal forests are more driven by changes in temperature. The NEE response to heat extremes in boreal forests still poses a challenge to modelers. Also, the response in boreal regions is likely to vary considerably with season. Breaking down the anomalies by season might yield some insight into the sources of variation among the models, and should be the topic of future work.

Currently, model intercomparison and benchmarking studies often focus on annual averages, seasonal cycles, or a general measure of interannual variability [*Randerson et al.*, 2009; *Kelley et al.*, 2013; *Piao et al.*, 2013; *Schwalm et al.*, 2013]. Recent studies identified droughts as the main driver for extreme decreases in GPP [*Reichstein et al.*, 2013; *Zscheischler et al.*, 2014a, 2014b], which is in good agreement with our results here. Using all three terrestrial carbon fluxes provided by the model environment we show that the impacts of climate extremes on GPP and TR can either compound or compensate each other (Figure 3), impeding an easy translation of GPP impacts into changes in the net carbon balance [cf. *Zscheischler et al.*, 2014a].

If processes are only marginally incorrectly represented in models, this can translate into inaccurate representations of higher order moments and extreme events. Equifinality in models [*Beven and Freer*, 2001; *Tang and Zhuang*, 2008] due to too few data constraints poses challenges to modelers and exacerbates finding the right parameter settings. Including explicit representations of the impacts of extreme climate events will help constrain carbon flux extremes and reduce equifinality.

References

Ahlström, A., G. Schurgers, A. Arneth, and B. Smith (2012), Robustness and uncertainty in terrestrial ecosystem carbon response to CMIP5 climate change projections, *Environ. Res. Lett.*, *7*(4), 044008.

Amiro, B. D., et al. (2010), Ecosystem carbon dioxide fluxes after disturbance in forests of North America, *J. Geophys. Res.*, *115*, G00K02, doi:10.1029/2010JG001390.

Anderegg, W. R. L., L. Plavcová, L. D. L. Anderegg, U. G. Hacke, J. A. Berry, and C. B. Field (2013), Drought's legacy: Multiyear hydraulic deterioration underlies widespread aspen forest die-off and portends increased future risk, *Global Change Biol.*, *19*(4), 1188–1196.

Anderson-Teixeira, K. J., J. P. Delong, A. M. Fox, D. A. Brese, and M. E. Litvak (2011), Differential responses of production and respiration to temperature and moisture drive the carbon balance across a climatic gradient in New Mexico, *Global Change Biol.*, *17*(1), 410–424.

Baldocchi, D. (2008), Turner Review No. 15. "Breathing"of the terrestrial biosphere: Lessons learned from a global network of carbon dioxide flux measurement systems, *Aust. J. Bot.*, *56*(1), 1–26.

Baldocchi, D., et al. (2001), Fluxnet: A new tool to study the temporal and spatial variability of ecosystem-scale carbon dioxide, water vapor, and energy flux densities, *Bull. Am. Meteorol. Soc.*, *82*(11), 2415–2434.

Bauweraerts, I., M. Ameye, T. M. Wertin, M. A. McGuire, R. O. Teskey, and K. Steppe (2014), Water availability is the decisive factor for the growth of two tree species in the occurrence of consecutive heat waves, *Agric. For. Meteorol.*, *189*, 19–29.

Beer, C., et al. (2010), Terrestrial gross carbon dioxide uptake: Global distribution and covariation with climate, *Science*, *329*(5993), 834–838.

Berry, J., and O. Bjorkman (1980), Photosynthetic response and adaptation to temperature in higher plants, *Annu. Rev. Plant Physiol.*, *31*(1), 491–543.

Beven, K., and J. Freer (2001), Equifinality, data assimilation, and uncertainty estimation in mechanistic modelling of complex environmental systems using the glue methodology, *J. Hydrol.*, *249*(1), 11–29.

Brando, P. M., D. C. Nepstad, E. A. Davidson, S. E. Trumbore, D. Ray, and P. Camargo (2008), Drought effects on litterfall, wood production and belowground carbon cycling in an Amazon forest: Results of a throughfall reduction experiment, *Philos. Trans. R. Soc. London, Ser. B*, *363*(1498), 1839–1848.

Burroughs, W. (2003), *Climate: Into the 21st century*, Cambridge Univ. Press, Cambridge, U. K.

Chapin, F., III et al. (2006), Reconciling carbon-cycle concepts, terminology, and methods, *Ecosystems*, *9*(7), 1041–1050.

Ciais, P., et al. (2005), Europe-wide reduction in primary productivity caused by the heat and drought in 2003, *Nature*, *437*(7058), 529–533.

Clark, D. A. (2004), Sources or sinks? The responses of tropical forests to current and future climate and atmospheric composition, *Philos. Trans. R. Soc. London, Ser. B*, *359*(1443), 477–491.

Clark, D. B., D. A. Clark, and S. F. Oberbauer (2010), Annual wood production in a tropical rain forest in NE Costa Rica linked to climatic variation but not to increasing CO2, *Global Change Biol.*, *16*(2), 747–759.

Corlett, R. T. (2011), Impacts of warming on tropical lowland rainforests, *Trends Ecol. Evol.*, *26*(11), 606–613.

Fischer, E., U. Beyerle, and R. Knutti (2013), Robust spatially aggregated projections of climate extremes, *Nat. Clim. Change*, *3*(12), 1033–1038.

Friedlingstein, P., et al. (2006), Climate-carbon cycle feedback analysis: Results from the C4MIP model intercomparison, *J. Clim.*, *19*(14), 3337–3353.

Handmer, J., et al. (2012), Changes in impacts of climate extremes: Human systems and ecosystems, in *Managing the Risks of Extreme Events and Disasters to Advance Climate Change Adaptation (IPCC SREX Report)*, edited by C. B. Field et al., pp. 231–290, Cambridge Univ. Press, Cambridge, U. K., and New York.

Hansen, J., M. Sato, and R. Ruedy (2012), Perception of climate change, *Proc. Natl. Acad. Sci.*, *109*(37), E2415–E2423.

Hartmann, H., W. Ziegler, and S. Trumbore (2013), Lethal drought leads to reduction in nonstructural carbohydrates in Norway spruce tree roots but not in the canopy, *Funct. Ecol.*, *27*, 413–427.

Hayes, D., and D. Turner (2012), The need for "apples-to-apples" comparisons of carbon dioxide source and sink estimates, *Eos, Trans. AGU*, *93*(41), 404–405.

(EaSM), DOE National Institute for Climate Change Research, USDA AFRI Program, and EPA STAR program. (LPJ-wsl) This work was conducted at LSCE, France, using a modified version of LPJ version 3.1 model, originally made available by the Potsdam Institute for Climate Impact Research. ORCHIDEE (Organizing Carbon and Hydrology In Dynamic Ecosystems) is a global land surface model developed at the IPSL (Institut Pierre Simon Laplace) in France. The simulations were performed with the support of the GhG Europe FP7 grant with computing facilities provided by LSCE (Laboratoire des Sciences du Climat et de l'Environnement) or TGCC (Très Grand Centre de Calcul). VISIT was developed at the National Institute of Environmental Studies, Japan. This work was mostly conducted during a visiting stay at Oak Ridge National Laboratory.

Holmgren, M., M. Hirota, E. H. van Nes, and M. Scheffer (2013), Effects of interannual climate variability on tropical tree cover, *Nat. Clim. Change*, *3*, 755–758.

Huntzinger, D., et al. (2012), North American carbon program (NACP) regional interim synthesis: Terrestrial biospheric model intercomparison, *Ecol. Modell.*, *232*, 144–157.

Huntzinger, D. N., et al. (2013), The North American carbon program Multi-Scale Synthesis and Terrestrial Model Intercomparison Project—Part 1: Overview and experimental design, *Geosci. Model Dev.*, *6*(6), 2121–2133.

Ito, A., and M. Inatomi (2012), Water-use efficiency of the terrestrial biosphere: A model analysis focusing on interactions between the global carbon and water cycles, *J. Hydrometeorol.*, *13*(2), 681–694.

Jain, A. K., H. S. Kheshgi, and D. J. Wuebbles (1996), A globally aggregated reconstruction of cycles of carbon and its isotopes, *Tellus B*, *48*(4), 583–600.

Joetzjer, E., H. Douville, C. Delire, P. Ciais, B. Decharme, and S. Tyteca (2013), Hydrologic benchmarking of meteorological drought indices at interannual to climate change timescales: A case study over the Amazon and Mississippi river basins, *Hydrol. Earth Syst. Sci.*, *17*(12), 4885–4895.

Jones, C., et al. (2013), 21st century compatible CO2 emissions and airborne fraction simulated by CMIP5 Earth system models under 4 representative concentration pathways, *J. Clim.*, *26*, 4398–4413.

Keenan, T., et al. (2012), Terrestrial biosphere model performance for inter-annual variability of land-atmosphere CO_2 exchange, *Global Change Biol.*, *18*(6), 1971–1987.

Kelley, D., I. C. Prentice, S. Harrison, H. Wang, M. Simard, J. Fisher, and K. Willis (2013), A comprehensive benchmarking system for evaluating global vegetation models, *Biogeosciences*, *10*(5), 3313–3340.

Koven, C. D., B. Ringeval, P. Friedlingstein, P. Ciais, P. Cadule, D. Khvorostyanov, G. Krinner, and C. Tarnocai (2011), Permafrost carbon-climate feedbacks accelerate global warming, *Proc. Natl. Acad. Sci.*, *108*(36), 14,769–14,774.

Krinner, G., N. Viovy, N. de Noblet-Ducoudré, J. Ogée, J. Polcher, P. Friedlingstein, P. Ciais, S. Sitch, and I. C. Prentice (2005), A dynamic global vegetation model for studies of the coupled atmosphere-biosphere system, *Global Biogeochem. Cycles*, *19*(1), GB1015, doi:10.1029/2003GB002199.

Law, B., F. Kelliher, D. Baldocchi, P. Anthoni, J. Irvine, D. v. Moore, and S. Van Tuyl (2001), Spatial and temporal variation in respiration in a young ponderosa pine forest during a summer drought, *Agric. For. Meteorol.*, *110*(1), 27–43.

Le Quéré, C., et al. (2013), The global carbon budget 1959–2011, *Earth Syst. Sci. Data*, *5*, 165–185.

Leonard, M., et al. (2013), A compound event framework for understanding extreme impacts, *WIREs Clim Change*, *5*, 113–128, doi:10.1002/wcc.252.

Li, H., M. Huang, M. S. Wigmosta, Y. Ke, A. M. Coleman, L. R. Leung, A. Wang, and D. M. Ricciuto (2011), Evaluating runoff simulations from the Community Land Model 4.0 using observations from flux towers and a mountainous watershed, *J. Geophys. Res.*, *116*, D24120, doi:10.1029/2011JD016276.

Lloyd-Hughes, B. (2012), A spatio-temporal structure-based approach to drought characterisation, *Int. J. Climatol.*, *32*(3), 406–418.

Mahecha, M. D., et al. (2010), Global convergence in the temperature sensitivity of respiration at ecosystem level, *Science*, *329*(5993), 838–840.

Mao, J., P. E. Thornton, X. Shi, M. Zhao, and W. M. Post (2012), Remote sensing evaluation of CLM4 GPP for the period 2000–09*, *J. Clim.*, *25*(15), 5327–5342.

McDowell, N. G. (2011), Mechanisms linking drought, hydraulics, carbon metabolism, and vegetation mortality, *Plant Physiol.*, *155*(3), 1051–1059.

McGuire, A. D., et al. (2009), Sensitivity of the carbon cycle in the Arctic to climate change, *Ecol. Monogr.*, *79*(4), 523–555.

McKee, T. B., N. J. Doesken, and J. Kleist (1993), The relationship of drought frequency and duration to time scales, in *Proceedings of the 8th Conference of Applied Climatology, 17–22 January, Anaheim, CA*, pp. 179–183, American Meterological Society, Boston, Mass.

Meir, P., D. Metcalfe, A. Costa, and R. Fisher (2008), The fate of assimilated carbon during drought: Impacts on respiration in Amazon rainforests, *Philos. Trans. R. Soc. London, Ser. B*, *363*(1498), 1849–1855.

Mora, C., et al. (2013), The projected timing of climate departure from recent variability, *Nature*, *502*(7470), 183–187.

Mueller, B., and S. I. Seneviratne (2012), Hot days induced by precipitation deficits at the global scale, *Proc. Natl. Acad. Sci.*, *109*(31), 12,398–12,403.

Nemani, R. R., C. D. Keeling, H. Hashimoto, W. M. Jolly, S. C. Piper, C. J. Tucker, R. B. Myneni, and S. W. Running (2003), Climate-driven increases in global terrestrial net primary production from 1982 to 1999, *Science*, *300*(5625), 1560–1563.

Phillips, O. L., et al. (2010), Drought-mortality relationships for tropical forests, *New Phytol.*, *187*(3), 631–646.

Piao, S., et al. (2013), Evaluation of terrestrial carbon cycle models for their response to climate variability and to CO2 trends, *Global Change Biol.*, *19*, 2117–2132.

Raczka, B. M., et al. (2013), Evaluation of continental carbon cycle simulations with North American flux tower observations, *Ecol. Monogr.*, *83*, 531–556.

Randerson, J. T., et al. (2009), Systematic assessment of terrestrial biogeochemistry in coupled climate-carbon models, *Global Change Biol.*, *15*(10), 2462–2484.

Rastetter, E. B. (2011), Modeling coupled biogeochemical cycles, *Front. Ecol. Environ.*, *9*(1), 68–73.

Reichstein, M., et al. (2013), Climate extremes and the carbon cycle, *Nature*, *500*(7462), 287–295.

Ricciuto, D. M., A. W. King, D. Dragoni, and W. M. Post (2011), Parameter and prediction uncertainty in an optimized terrestrial carbon cycle model: Effects of constraining variables and data record length, *J. Geophys. Res.*, *116*, G01033, doi:10.1029/2010JG001400.

Rustad, L., G. Campbell, G. Marion, R. Norby, M. Mitchell, A. Hartley, J. Cornelissen, J. Gurevitch, and GCTE-News (2001), A meta-analysis of the response of soil respiration, net nitrogen mineralization, and aboveground plant growth to experimental ecosystem warming, *Oecologia*, *126*(4), 543–562.

Schaefer, K., T. Zhang, L. Bruhwiler, and A. P. Barrett (2011), Amount and timing of permafrost carbon release in response to climate warming, *Tellus B*, *63*(2), 165–180.

Schneider von Deimling, T., M. Meinshausen, A. Levermann, V. Huber, K. Frieler, D. Lawrence, and V. Brovkin (2012), Estimating the near-surface permafrost-carbon feedback on global warming, *Biogeosciences*, *9*(2), 649–665.

Schwalm, C. R., et al. (2010), Assimilation exceeds respiration sensitivity to drought: A fluxnet synthesis, *Global Change Biol.*, *16*(2), 657–670.

Schwalm, C. R., et al. (2012), Reduction in carbon uptake during turn of the century drought in western North America, *Nat. Geosci.*, *5*(8), 551–556.

Schwalm, C. R., D. N. Huntinzger, A. M. Michalak, J. B. Fisher, J. S. Kimball, B. Mueller, K. Zhang, and Y. Zhang (2013), Sensitivity of inferred climate model skill to evaluation decisions: A case study using CMIP5 evapotranspiration, *Environ. Res. Lett.*, *8*(2), 024,028.

Seneviratne, S. I., T. Corti, E. L. Davin, M. Hirschi, E. B. Jaeger, I. Lehner, B. Orlowsky, and A. J. Teuling (2010), Investigating soil moisture-climate interactions in a changing climate: A review, *Earth Sci. Rev.*, *99*(3), 125–161.

Seneviratne, S. I., et al. (2012), Changes in climate extremes and their impacts on the natural physical environment, in *Managing the Risks of Extreme Events and Disasters to Advance Climate Change Adaptation (IPCC SREX Report)*, edited by C. B. Field et al., pp. 109–230, Cambridge Univ. Press, Cambridge, U. K., and New York.

Shi, X., J. Mao, P. E. Thornton, F. M. Hoffman, and W. M. Post (2011), The impact of climate, CO2, nitrogen deposition and land use change on simulated contemporary global river flow, *Geophys. Res. Lett.*, *38*, L08704, doi:10.1029/2011GL046773.

Sillmann, J., V. Kharin, F. Zwiers, X. Zhang, and D. Bronaugh (2013), Climate extreme indices in the CMIP5 multi-model ensemble. Part 2: Future climate projections, *J. Geophys. Res. Atmos.*, *118*, 2473–2493, doi:10.1002/jgrd.50188.

Sitch, S., et al. (2003), Evaluation of ecosystem dynamics, plant geography and terrestrial carbon cycling in the LPJ dynamic global vegetation model, *Global Change Biol.*, *9*(2), 161–185.

Smith, M. D. (2011), An ecological perspective on extreme climatic events: A synthetic definition and framework to guide future research, *J. Ecol.*, *99*(3), 656–663.

Stroeve, J. C., V. Kattsov, A. Barrett, M. Serreze, T. Pavlova, M. Holland, and W. N. Meier (2012), Trends in arctic sea ice extent from CMIP5, CMIP3 and observations, *Geophys. Res. Lett.*, *39*, L16502, doi:10.1029/2012GL052676.

Tang, J., and Q. Zhuang (2008), Equifinality in parameterization of process-based biogeochemistry models: A significant uncertainty source to the estimation of regional carbon dynamics, *J. Geophys. Res.*, *113*, G04010, doi:10.1029/2008JG000757.

Thornton, P., et al. (2002), Modeling and measuring the effects of disturbance history and climate on carbon and water budgets in evergreen needleleaf forests, *Agric. For. Meteorol.*, *113*(1), 185–222.

Tian, H., X. Xu, C. Lu, M. Liu, W. Ren, G. Chen, J. Melillo, and J. Liu (2011), Net exchanges of CO_2, CH_4, and N_2O between China's terrestrial ecosystems and the atmosphere and their contributions to global climate warming, *J. Geophys. Res.*, *116*, G02011, doi:10.1029/2010JG001393.

Tian, H., et al. (2012), Century-scale responses of ecosystem carbon storage and flux to multiple environmental changes in the southern United States, *Ecosystems*, *15*(4), 674–694.

von Liebig, J. (1847), *Chemistry in Its Applications to Agriculture and Physiology*, Taylor and Walton, London, U. K.

Wang, W., et al. (2013), Variations in atmospheric CO2 growth rates coupled with tropical temperature, *Proc. Natl. Acad. Sci.*, *110*(32), 13,061–13,066.

Wei, Y., et al. (2013), The North American carbon program multi-scale synthesis and terrestrial model intercomparison project: Part 2—Environmental driver data, *Geosci. Model Dev. Discuss.*, *6*, 5375–5422.

Wu, Z., P. Dijkstra, G. W. Koch, J. Penuelas, and B. A. Hungate (2011), Responses of terrestrial ecosystems to temperature and precipitation change: A meta-analysis of experimental manipulation, *Global Change Biol.*, *17*(2), 927–942.

Zeng, N., A. Mariotti, and P. Wetzel (2005), Terrestrial mechanisms of interannual CO_2 variability, *Global Biogeochem. Cycles*, *19*(1), GB1016, doi:10.1029/2004GB002273.

Zhao, M., and S. W. Running (2010), Drought-induced reduction in global terrestrial net primary production from 2000 through 2009, *Science*, *329*(5994), 940–943.

Zscheischler, J., M. D. Mahecha, S. Harmeling, and M. Reichstein (2013), Detection and attribution of large spatiotemporal extreme events in Earth observation data, *Ecol. Inf.*, *15*, 66–73.

Zscheischler, J., M. D. Mahecha, J. von Buttlar, S. Harmeling, M. Jung, A. Rammig, J. T. Randerson, B. Schölkopf, S. I. Seneviratne, and E. Tomelleri (2014a), A few extreme events dominate global interannual variability in gross primary production, *Environ. Res. Lett.*, *9*, 035001.

Zscheischler, J., M. Reichstein, S. Harmeling, A. Rammig, E. Tomelleri, and M. D. Mahecha (2014b), Extreme events in gross primary production: A characterization across continents, *Biogeosciences*, *11*, 2909–2924, doi:10.5194/bg-11-2909-2014.